Integrated Fuzzy Guidance Law for High Maneuvering Targets Based on Proportional Navigation Guidance

L. Hassan*, S. H. Sadati* (C.A.) and J. Karimi*

Abstract: An Integrated Fuzzy Guidance (IFG) law for a surface to air homing missile is introduced. The introduced approach is a modification of the well-known Proportional Navigation Guidance (PNG) law. The IFG law enables the missile to approach a high maneuvering target while trying to minimize control effort as well as miss distance in a two-stage flight. In the first stage, while the missile is far from the intended target, the IFG tends to have low sensitivity to the target maneuvering seeking to minimize the overall control effort. When the missile gets closer to the target, a second stage is started and IFG law changes tactic by increasing that sensitivity attempting to minimize the miss distance. A Fuzzy-Switching Point (FSP) controller manages the transition between the two stages. The FSP is optimized based on variety of scenarios; some of which are discussed in the paper. The introduced scheme depends on line-of-sight angle rate, closing velocity, and target-missile relative range. The performance of the new IFG law is compared with other guidance laws. The results show a relative superiority in wide variety of flight conditions.

Keywords: Fuzzy Logic, Homing Missile, Proportional Navigation Guidance.

1 Introduction

Developing appropriate guidance laws has attracted considerable attentions. This mainly emerges in the case of highly maneuverable aircrafts, for which conventional approaches may not be sufficient to obtain both tracking and interception, unless there is a perfect knowledge about the system dynamics and also extensive computational capabilities are available. The conventional approaches to this subject include: Exact feedback linearization [1, 2], Sliding mode control [3, 4], Adaptive control [5, 6], and the last not the least LQ-based control system [7, 8]. It is therefore appropriate to investigate other advanced control theories to improve existing performance capabilities. In this line of thought, Fuzzy logic controllers have shown to exhibit suitable properties which help eliminating measurement deficiencies or other difficulties such as changing climatic conditions. This could help open a new approach for control system design.

In fact; most fuzzy guidance laws are implemented based on the well-known classical guidance laws; especially PNG law which enjoys simplicity, effectiveness and ease of implementation [9-12]. In general, PNG controller remains a good choice against low maneuvering targets [13], while such approach cannot provide satisfactory performance and robustness with respect to high maneuvering targets and results large value of M_D because of dynamic saturation at the end game [14]. Designers solve this problem by modifying the PNG law to an Augmented Proportional Navigation Guidance (APNG) one. This is achieved by adding a term of the target acceleration into the PNG law, the matter that enables PNG controller to be more effective against highly maneuvering targets. On the other hand, adding the corresponding term means that the target's acceleration has to be estimated instantaneously. To overcome this difficulty an integrated fuzzy guidance controller namely IFG is proposed. It is based on the concept of PNG law and consists of two autonomous fuzzy controllers. Each of the two controllers has its own characteristics; together they can achieve the interception. A FSP controller is designed to switch between the two fuzzy controllers. The first fuzzy controller namely FG1 is designed to be with low sensitivity to the target maneuvering trying to minimize the control effort (C_{EFF}) and would be used in the first stage of flight where the missile is far from its target. Whereas, the second fuzzy controller, denoted by FG2, is designed to have higher sensitivity to target's maneuvering trying to minimize the miss distance (M_D) when the missile becomes closer to its target.

Iranian Journal of Electrical & Electronic Engineering, 2013.
Paper first received 11 Feb. 2013 and in revised form 6 Oct. 2013.
* The Authors are with the department of Aerospace Engineering, Maleke Ashtar University of Technology. Tehran, Iran.
E-mails: lab.has77@yahoo.com, hsadati@aut.ac.com and karimi_j@alum.sharif.edu.

The paper is organized as follows: We proceed with a brief overview of the PNG law in Section 2, whereas; IFG controller with its three components FG1, FG2, and FSP is explained in Section 3. We provide some case-studies in Section 4 and the differences of all guidance laws are discussed. Finally, in Section 5 we discuss some important conclusions.

2 An Overview to PNG Guidance Law

For problem formulation, we use point mass. The missile and target are moving with constant velocities where drag and gravitational effects are neglected. The engagement scenario is shown in Fig. 1, where λ, L and HE are; Line-Of-Sight (LOS) angle, lead angle and head angle respectively, whilst γ_M, γ_T, V_M, V_T, A_M and A_T are flight path angles, velocities, accelerations of the missile and the target, respectively. Also, A_C is the acceleration command of the missile. In addition, R_{TM1} and R_{TM2} are horizontal and vertical relative distances and R_{TM} is the relative target-missile distance.

In vertical plane, the closing velocity V_C which is negative rate of the target-missile range can be written as:

$$V_C = -\dot{R}_{TM} \cong V_M - V_T \tag{1}$$

where:

$$\dot{R}_{TM} = -\frac{R_{TM1}V_{TM1}+R_{TM2}V_{TM2}}{R_{TM}} \tag{2}$$

The LOS angle λ and its rate $\dot{\lambda}$ can be given as:

$$\lambda = \tan^{-1}\left(\frac{R_{TM1}}{R_{TM2}}\right) \tag{3}$$

$$\dot{\lambda} = \frac{R_{TM1}V_{TM2}-R_{TM2}V_{TM1}}{{R_{TM}}^2} \tag{4}$$

Theoretically; PNG as used in many missiles gives the commanded acceleration perpendicular to the instantaneous LOS, the magnitude being proportional to the LOS rate and the closing velocity as:

$$A_C = NV_C\dot{\lambda} \tag{5}$$

A missile employing PNG law usually aims toward expected interception point. Theoretically, a missile will reach its target if both of missile and the target continue flying along a straight-line path at constant velocities. However, this idealized assumption is violated for high maneuvering targets [15]. That is because of the rapid change of $\dot{\lambda}$ which happens as soon as the missile gets closer to its maneuvering target the matter could eventually lead to some form of dynamic saturation. A fuzzy controller is expected to provide a desirable solution through modifying PNG. This prevents such undesirable scenarios that would arise from unwanted system saturations.

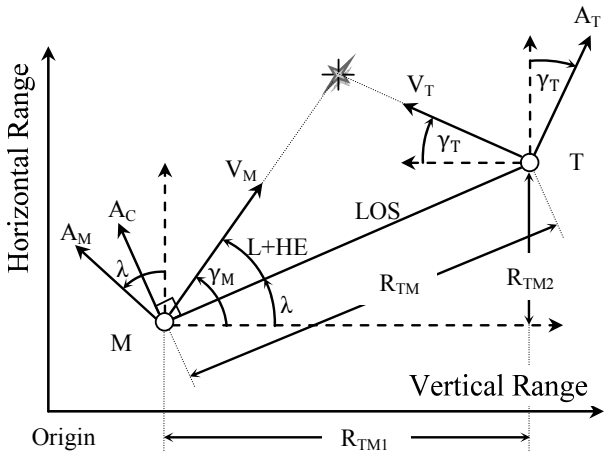

Fig. 1 Two-dimensional missile-target engagement geometry.

3 Architecture of Integrated Fuzzy Guidance (IFG) Law

The main idea behind the proposed IFG law is to use relatively small acceleration commands while the missile is far from the target, where high maneuvers would not achieve a better performance regarding a maneuvering target; so we prefer to save C_{EFF}. On the other hand, the acceleration command could be increased sensibly as soon as the missile gets closer to its target that is to deliver good tracking capability and to decrease M_D.

The entire proposed structure is shown in Fig. 2, with three main components; FG1, FG2, and FSP. The heart of the system is, in fact; the FSP controller which needs to be tuned to ensure smooth transition between FG1and FG2.

By assuming two weights w_1 and w_2, one can define how long any of FG1 and FG2 is engaged and how the transition between the two is moderated. Each controller FG1, FG2, and FSP has similar structure as illustrated in Fig. 3.

Fuzzy inference systems are composed of five functional blocks [16]. These are; a rule base containing a number of if-then rules, a database that defines the Membership Functions (MFs), a decision making interface which operates the given rules, a fuzzification interface that converts the crisp inputs into "degree of match" with the linguistic values such as small, large etc., and a defuzzification interface which reconverts to a crisp output.

Different case-studies reveal that for the current work, the Center of Area (CoA) method, which supplies defuzzified output with better continuity, is more effective [17, 18]. Furthermore; minimum Mamdani (AND method), the most popular inference engine, provides good results and allows easy and effective computation with real time capability [19, 20].

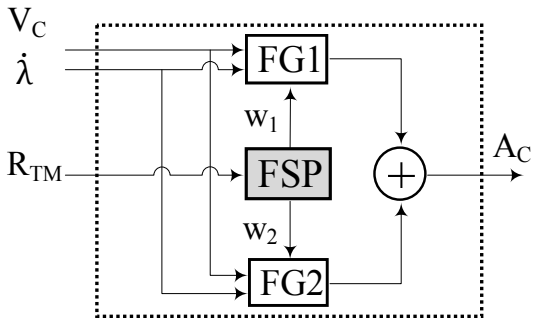

Fig. 2 The IFG controller.

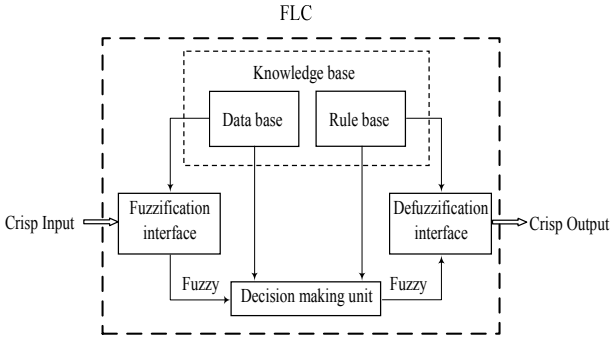

Fig. 3 Fuzzy inference system.

The first step to design a fuzzy controller is to choose number and shapes of the MFs for input and output. Actually; there is no rigid restrictions on the number of MFs. Determination of the number and the shape of MFs is a compromise between guidance accuracy and computation complexity.

In this work; three groups of MFs with triangular shape are investigated for each of FG1 and FG2. The triangular MFs give faster response. Using other more complex forms of MFs would not give any significant advantage over the triangular ones [21].

Similar to PNG law, the inputs of both controllers FG1 and FG2 are both V_C and $\dot{\lambda}$ whereas the output is A_C. Each controller exploits two groups of MFs corresponding to the inputs whereas the third group is used for the output. Each group has seven MFs whereas each MF is denoted by a linguistic value. The linguistic values can be represented as :{ LN, MN, SN, ZE, SP, MP, LP}, where "L", "M", and "S" represent "Large", "Medium", and "Small" respectively. Similarly; "N", "ZE", and "P" denote "Negative", "Zero", and "Positive" respectively.

The FSP controller receives R_{TM} as its input and gives two weights (w_1, w_2) on its outputs. The input in turn has two MFs; Small "S" and Large "L" with bell-shaped MFs to insure smooth transition whereas each output has two triangular MFs.

The data of each controller are normalized according to Max Method Normalization [22]. This method divides the performance ratings of each attribute (r) by its maximum performance rating (r_{max}). The normalization procedures are required to transform performance ratings with different data measurement units into a decision matrix with compatible unit. In the current design the maximum values are obtained based on the knowledge available about missile dynamic in addition to previous experiences about other classical guidance laws in the PNG's class.

Finally; the rules that organize the relationship between the control action and missile-target measurements have to be defined. Here; the rules are determined according to conception of the PNG law. In fact, the choice of proper MFs and rules requires a great deal of engineering intuition and so it is considered as some type of engineering art. More explanation of the process is improved in the next sections.

3.1 Search for Proper Rules

Fuzzy Logic, in the first glance, looks simple and straightforward; nonetheless, like every engineering process complexities arise as one proceed further into the design. This work is not an exception; here the aim is to find a set of proper rules that allow guiding a missile toward its target in a two-stage flight. One must note to the point that, both FG1 and FG2 have similar rules and MFs serve as input to them. The process to define the rules and the MFs is explained in the following statements.

With Eq. (5), the acceleration command A_C of PNG law is proportional to $\dot{\lambda}$ multiplied by V_C. Eq. (5) shows that sign of A_C remains negative when $\dot{\lambda}$ or V_C have opposite signs. This conception can be tabulated as shown in Table 1.

Before feeding into the controller, all data have to be normalized in the interval [-1, 1]. And everyone knows the fact; multiplication of two values in this interval will result a new value that is smaller than the smallest of them and it is closer to the smaller one. In addition; the value will be zero if any of them was zero. Adopting these concepts, the linguistic value A_C is defined as in Table 2.

Gathering the conceptions of Table 1 and Table 2, the rules can be tabulated as in Table 3.

These rules are, in fact, describing PNG law in a fuzzy domain and exhibit almost similar behavior to the PNG when using similar shapes of MFs for both inputs and output.

Table 1 Defining the sign of A_C.

If	V_C	Is	N	and	$\dot{\lambda}$	is	P	then	A_C	is	N
If	V_C	Is	N	and	$\dot{\lambda}$	is	N	then	A_C	is	P
If	V_C	Is	P	and	$\dot{\lambda}$	is	P	then	A_C	is	P
If	V_C	Is	P	and	$\dot{\lambda}$	is	N	then	A_C	is	N

Table 2 Defining the value of A_C.

If	V_C	Is	L	and	$\dot{\lambda}$	is	L	then	A_C	is	L
If	V_C	Is	L	and	$\dot{\lambda}$	is	M	then	A_C	is	M
If	V_C	Is	L	and	$\dot{\lambda}$	is	S	then	A_C	is	S
If	V_C	is	L	and	$\dot{\lambda}$	is	ZE	then	A_C	is	ZE
If	V_C	is	M	and	$\dot{\lambda}$	is	L	then	A_C	is	M
If	V_C	is	M	and	$\dot{\lambda}$	is	M	then	A_C	is	M
If	V_C	is	M	and	$\dot{\lambda}$	is	S	then	A_C	is	S
If	V_C	is	M	and	$\dot{\lambda}$	is	ZE	then	A_C	is	ZE
If	V_C	is	S	and	$\dot{\lambda}$	is	L	then	A_C	is	S
If	V_C	is	S	and	$\dot{\lambda}$	is	M	then	A_C	is	S
If	V_C	is	S	and	$\dot{\lambda}$	is	S	then	A_C	is	S
If	V_C	Is	S	and	$\dot{\lambda}$	is	ZE	then	A_C	is	ZE
If	V_C	Is	ZE	and	$\dot{\lambda}$	is	L	then	A_C	is	ZE
If	V_C	Is	ZE	and	$\dot{\lambda}$	is	M	then	A_C	is	ZE
If	V_C	Is	ZE	and	$\dot{\lambda}$	is	S	then	A_C	is	ZE
If	V_C	Is	ZE	and	$\dot{\lambda}$	is	ZE	then	A_C	is	ZE

Table 3 The rules.

A_C		$\dot{\lambda}$						
		LP	MP	SP	ZE	SN	MN	LN
V_C	LP	LP	MP	SP	ZE	SN	MN	LN
	MP	MP	MP	SP	ZE	SN	MN	MN
	SP	SP	SP	SP	ZE	SN	SN	SN
	ZE	ZE	ZE	ZE	ZE	ZE	ZE	ZE
	SN	SN	SN	SN	ZE	SP	SP	SP
	MN	MN	MN	SN	ZE	SP	MP	MP
	LN	LN	MN	SN	ZE	SP	MP	LP

3.2 Defining MFs

As mentioned previously, the controllers FG1 and FG2 have similar rules and similar input MFs. Since the rules are derived, the MFs of the inputs ($\dot{\lambda}$ and V_C) are adjusted using test and error method and plotted as shown in Fig. 4.

The last remained part is to investigate the output MFs under the consideration; FG1 has to ensure low sensitivity and FG2 has to ensure high sensitivity.

In this regard; FG1 is more sensitivity than FG2 when both controllers are fed with same input value and FG1 is able to give larger output value than FG2.

Actually, the output value can be controlled by three factors; shape of MFs, number of MFs, and CoA location. Investigations showed that CoA location has much more effecting among the other factors. So, the output value will be controlled by shifting the location of the CoA respect to Zero Point (ZP), where the increasing is achieved by displacing CoA far from ZP and decreasing is carried out by displacing it toward ZP. The following figured example demonstrates the process.

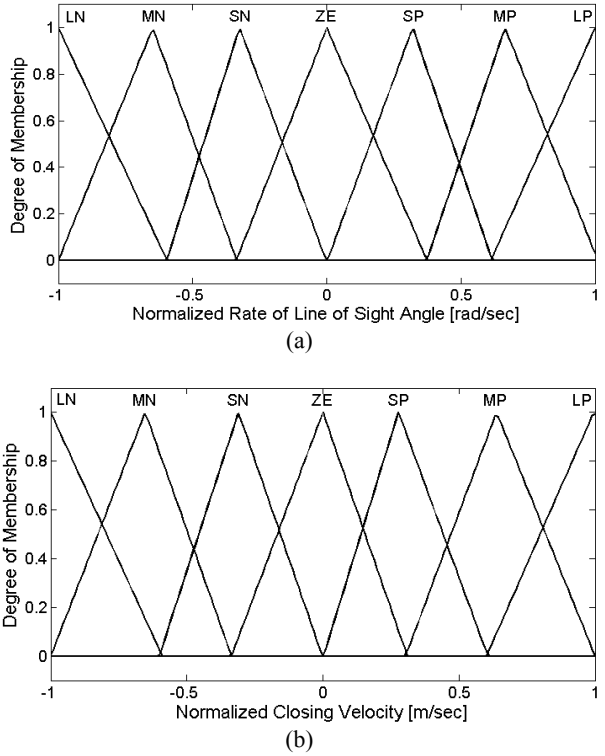

Fig. 4 Input MFs for both FG1 and FG2. (a) MFs of rate of LOS angle. (b) MFs of the closing velocity.

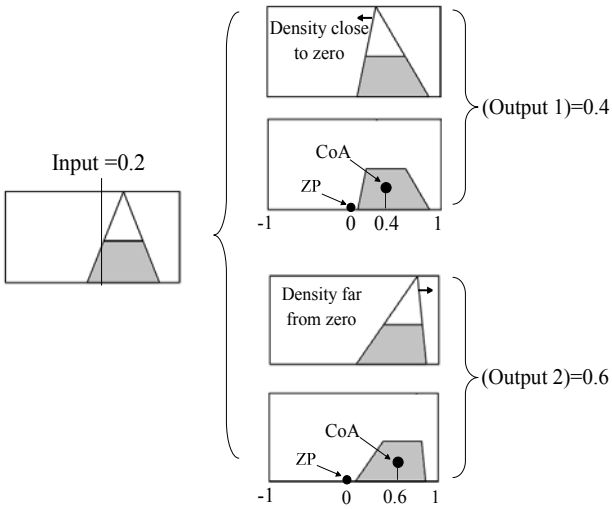

Fig. 5 CoA effecting on the output values.

With Fig. 5; suppose FG1 has output MF with density close to ZP whereas FG2 has output MF with density far from ZP. Feeding input value equals 0.2 for both controllers; FG1 gives output value equals 0.4 whereas FG2 gives output value equals 0.6. It is clear that for same input value, FG2 gives greater output value.

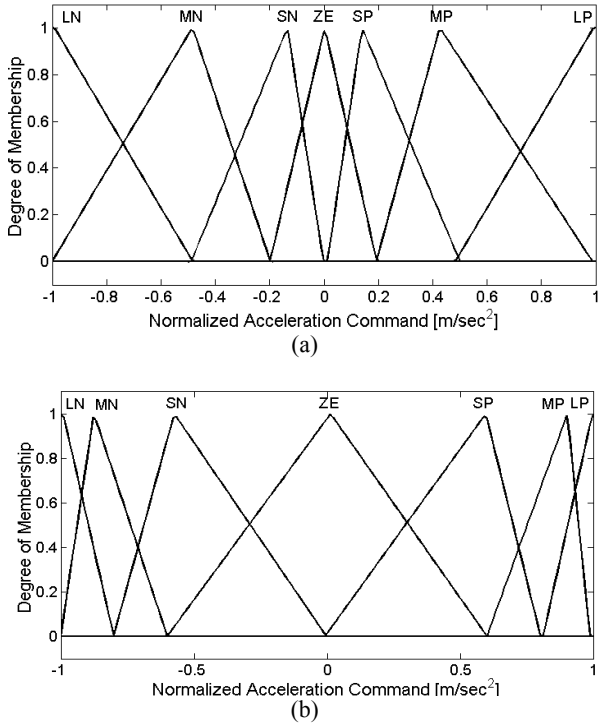

Fig. 6 Output MFs. (a) The output MFs of FG1 with density close to ZP. (b) The output MFs of FG2 with density far from ZP.

Based on the previous illustration; FG1 can be with low sensitivity by pressing the output MFs toward ZP which in turn shifts the CoA of each MF toward ZP and decreases the acceleration command values. In turn; decreasing the acceleration command leads to decrease the guidance law sensitivity the mater that causes C_{EFF} conserving.

On the other hand; spreading the output MFs of FG2 far from ZP leads to shift the CoA of each MF far from ZP and increases the acceleration command value which in turn increases the guidance law sensitivity, the mater that causes small M_D. Fig. 6 shows the output MFs for FG1 and FG2.

3.3 The FSP Controller

The FSP controller has single input R_{TM} and two outputs (w_1, w_2), the rules of this controller are simply determined as following:

- If R_{TM} is large then w_1 is large and w_2 is small.
- If R_{TM} is small then w_1 is small and w_2 is large.

The first rule refers to FG1 domination whereas the second rule refers to FG2 domination. The FSP insures the integration between the two controllers and balances the dominance of FG1 and FG2.

3.3.1 MFs of the FSP controller

The integration is achieved by transition from FG1 to FG2 via the weights w_1 and w_2. The weights in turn are changed respect to the input MFs which define the transition way. Since FG1 has to give low A_C values and FG2 has to give large ones, a sudden transition will force the missile to change maneuvering in high rates, this might cause target missing or even bending the missile body. MFs with broken shapes (e.g., Triangular) are the main reason of sudden change because of its corners, whereas MFs with smooth curves (e.g., Bell-shaped) can avoid the hasty transition. So, Bell-shaped MFs are used for FSP input. Since the input MFs insure the smooth transition between w_1 and w_2, both of the weights have to insure the exact values "0" and "1", otherwise, undesirable coupling between FG1 and FG2 will happen.

Anyway, we the smooth transition will be discussed in a separate section whilst the ability of insuring the exact values "0" and "1" will be shown currently.

Actually, the exact values "0" and "1" are achieved by adjusting output triangular MFs as close as possible to the terminals, therein the values "0" and "1" are located (e.g., "Fig. 5").

It is notable to point that, an opposite result occurs when expanding the MFs far from the terminals, where the output values become somewhat more than "0" or less than "1", the matter that causes undesirable mix between FG1 and FG2 before or after switching.

Fig. 7, which plotted as an example, shows how the adjusting close to the terminals can insure the exact values "0" or "1". In the drawing, it is considered that, for the input ($R_{TM} = 0.7$), the switching from FG1 to FG2 is completed. So that, it supposed to have complete-inert FG1 and complete-energetic FG2.

Case (a) shows that the MFs are not adjusted close to terminals. Therefore, the outputs are $w_1 = 0.2$ and $w_2 = 0.8$, this means a coupling still existent between FG1 and FG2 even after finishing the transition. By adjusting the MFs close to terminals, as shown in Case (b), the outputs become equal "0" and "1" respectively, ensuring no-coupling (complete-inert and complete-energetic).

3.3.2 Optimizing Input MFs

Since we insured the undesirable coupling, it is turn to achieve an optimal transition using the input Bell-shaped MFs. In fact; the generalized MFs depends on three parameters **a**, **b**, and **c**, given as following:

$$f(\mathbf{x}, \mathbf{a}, \mathbf{b}, \mathbf{c}) = \frac{1}{1+\left|\frac{\mathbf{x}-\mathbf{c}}{\mathbf{a}}\right|^{2\mathbf{b}}} \quad (6)$$

where; **x** denotes degree of the MF, **a** controls the width of the curve, **b** controls its slope and **c** control its center. The transition between the two controllers appears clearly in Fig. 8. Before transition, FG1 is complete-energetic and FG2 is complete-inert, therein; $w_1 = 1$ and $w_2 = 0$. When switching starts, FG2 begins to share FG1 smoothly whilst FG1 remains dominator. In this interval w_1 decreases and w_2 increases until the weights become equal each to other at Point (**P**).

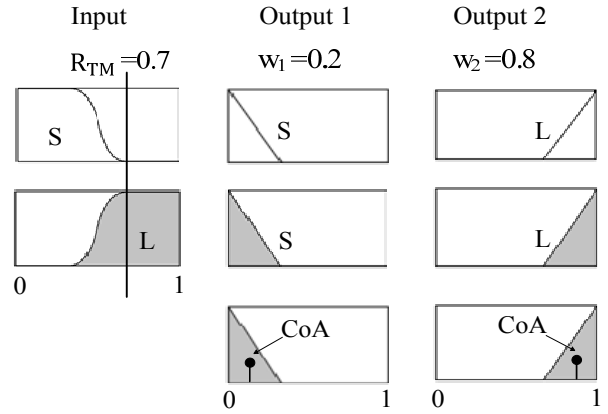

Case (a) MFs adjusting far from terminals

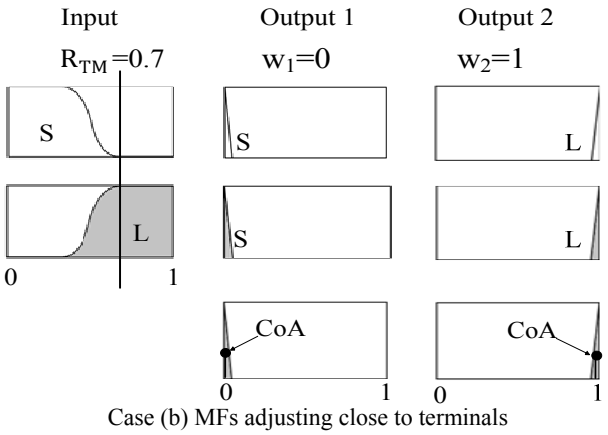

Case (b) MFs adjusting close to terminals

Fig. 7 MFs adjusting respect to the terminals.

Thereafter, the process is reversed and FG2 becomes dominator. The process continues till $w_1 = 0$ and $w_2 = 1$, thereon the switching is completed.

The location of **P** and the slope of the MFs are managing the entire work of the IFG controller and the best tuning of these MFs the best performance of the IFG controller. For this purpose, an algorithm using MatLab software is investigated.

The algorithm has two main steps; in the first one we define when the transition will be, upon that the algorithm shifts the location of **P** which recognized by the parameters (**a**, **c**). Whereas the assessment of the slope is achieved in the next step based on the parameter (**b**) that defines how the transition will be. The parameters (**a**, **b**, and **c**) are updated using sweep method. Fig. 9 illustrates the overall process of the algorithm.

The algorithm is run for variety different scenarios of target maneuvering. In each scenario the minimum value of the objective function is calculated. The calculated value and its corresponding parameters are saved. All saved values of the object functions are compared. The parameters that cause smallest value of the object function among all scenarios are extracted as an optimal solution.

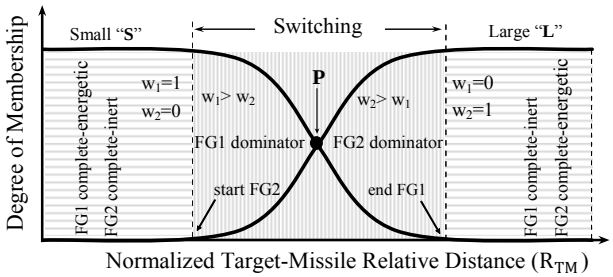

Fig. 8 MFs of input.

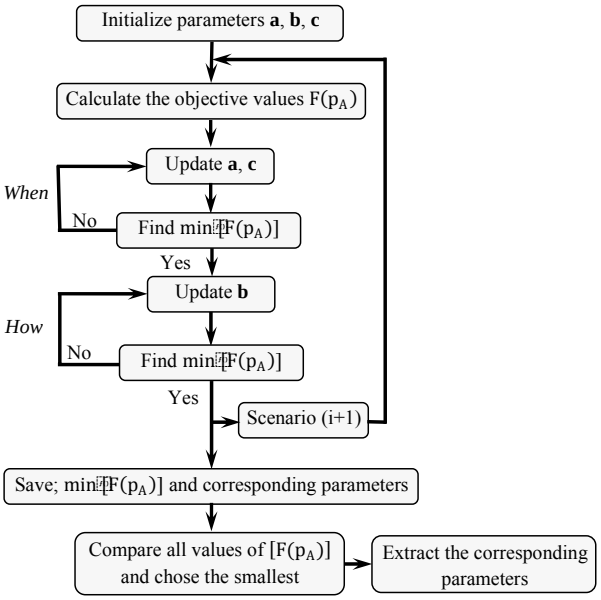

Fig. 9 Flowchart of the optimization algorithm.

The object function includes two terms; C_{EFF} and M_D and calculated as following:

$$F(p_A) = k_1 . \int_0^{t_f} {A_C}^2 dt + k_2 . R_{TM}(t_f) \quad (7)$$

where p_A is the array's parameters needed to be optimized, t_f is the entire time of flight, k_1 and k_2 are designed constants refer to the terms preference C_{EFF} and M_D. In the current design, same importance for the terms is considered, so that; $k_1 = 1/A_{C_{max}}$, $k_2 = 1/R_{TM(t_f)_{max}}$, where $A_{C_{max}}$ and $R_{TM(t_f)_{max}}$ are the maximum allowable values of the acceleration and the miss distance respectively.

Running the simulation for variety of extreme scenarios, the algorithm calculates the optimal parameters of FSP controller. The parameters are extracted and listed as shown in Table 4.

Table 4 Tuned parameters of the FSP.

MFs	a	b	C
S	0.508	8.31	-0.15
L	0.507	8.29	0.85

4 Results and Analysis

During simulation, the following considerations are provided: The initial positions of the target and the missile are $(0, 0)$ km, $(8, 3)$ km, respectively. Also, $V_M = 1000\ (m.sec^{-1})$ and $V_T = 300\ (m.sec^{-1})$. The target can accelerate within $[-3,\ 8]g$, whereas the missile can accelerate within $[-20, 20]g$, where $g = 9.8(m.sec^{-2})$ is the gravity constant. The navigation ratio of PNG law is $N = 4$.

The general arrangement of the guidance loop is illustrated in Fig. 10. With the help of [23], the transfer function of Flight Control System (FCS) and the plant is presented as:

$$\frac{A_M}{A_C} = \frac{-0.006S^2+11.296}{0.003S^3+0.139S^2+3.42S+11.313} \quad (8)$$

Since the acceleration command is perpendicular to the LOS vector as shown in Fig. 1, and only command forces perpendicular to the missile body can be applied, Eq. (8) is derived assuming that the missile velocity vector is aligned with the missile body.

One of the important factors in the simulation process is usually the integration time-step. This is normally chosen based on nature of the problem or experience. Here, a time step equals 0.01 second is used, mainly because a typical missile-gyro gyrates around 100 cycles per second. Additional important factor is that simulation stop condition; with Eq. (1), one can note that V_C will be zero when R_{TM} that denotes the resulting M_D is extrumum (e.g., the function is either minimum or maximum when its derivative is zero), therein the simulation will stop.

To complete the work, the maximum values needed for normalizing are simply calculated basing on Eq. (1) as well as Eq. (5) and tabulated as shown in Table 5.

Table 5 Maximum values for normalization.

Substantives	Calculated	Max values
$\mathbf{A_C}$	20×9.8	197 [m/sec^2]
$\mathbf{V_C}$	$1000 + 300$	1300 [m/sec]
$\dot{\boldsymbol{\lambda}}$	$(20 \times 9.8)/(4 \times 1300)$	0.038 [rad/sec]

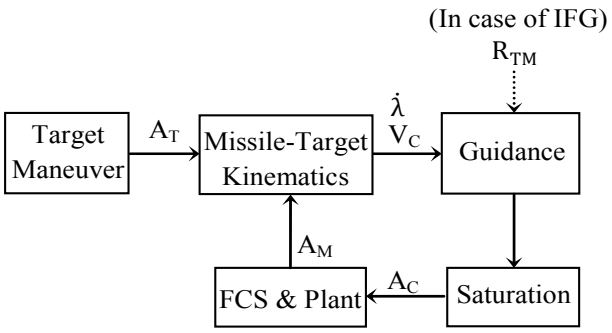

Fig. 10 Homing Guidance Loop.

Since there is no ability to examine the resulted guidance laws for all possible scenarios in the plane, engagement accuracy of the previous guidance laws against 24 different scenarios is examined. The scenarios are simulated respect to the target acceleration $A_T = [-3, -2, \ldots, 7, 8]g$, as well as its movement direction (incoming or evading). Since there is no ability to show all scenarios, four selected scenarios respect to maximum capability of the target maneuvering are chosen and plotted as shown in Fig. 11.

The selected scenarios are achieved for the following target maneuvering styles; Incoming Up-ward, Incoming Down-ward, Evading Up-ward, and Evading Down-ward. Fig. 11 shows that using PNG or IFG enables to intercept the maneuvering target. In addition it shows that even using FG1 or FG2 can insure the interception regardless of the resulting M_D or C_{EFF}.

The acceleration histories, respects to each selected scenario, are separately illustrated as shown in Fig. 12. With Fig. 12, acceleration command histories show that the saturation might happen during the endgame for PNG as Fig. 12-(a, b, c), the matter that causes M_D increasing. Also it displays the smooth transition from FG1 to FG2.

The Root-Mean-Square values (RMS) for the overall 24 scenarios are listed in Table 6. This table shows that the FG1law conserves the C_{Eff} more than the other ones, nonetheless; it gives the highest M_D. On the other hand, the table shows that the FG2 law causes the smallest M_D, but leads to higher C_{Eff}.

The most interesting outcome, which results from integrating both controllers by the optimized FSP, is the IFG law which overcomes the PNG law in terms of M_D and C_{Eff} together, not alike FG1 or FG2 those achieve overcoming in one of the two terms. Fig. 13, plots the resulting, M_D and C_{Eff} for the overall 24 scenarios in details.

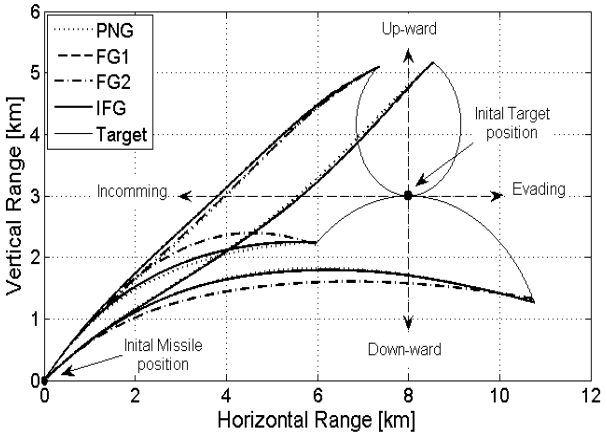

Fig. 11 Trajectories of selected scenarios.

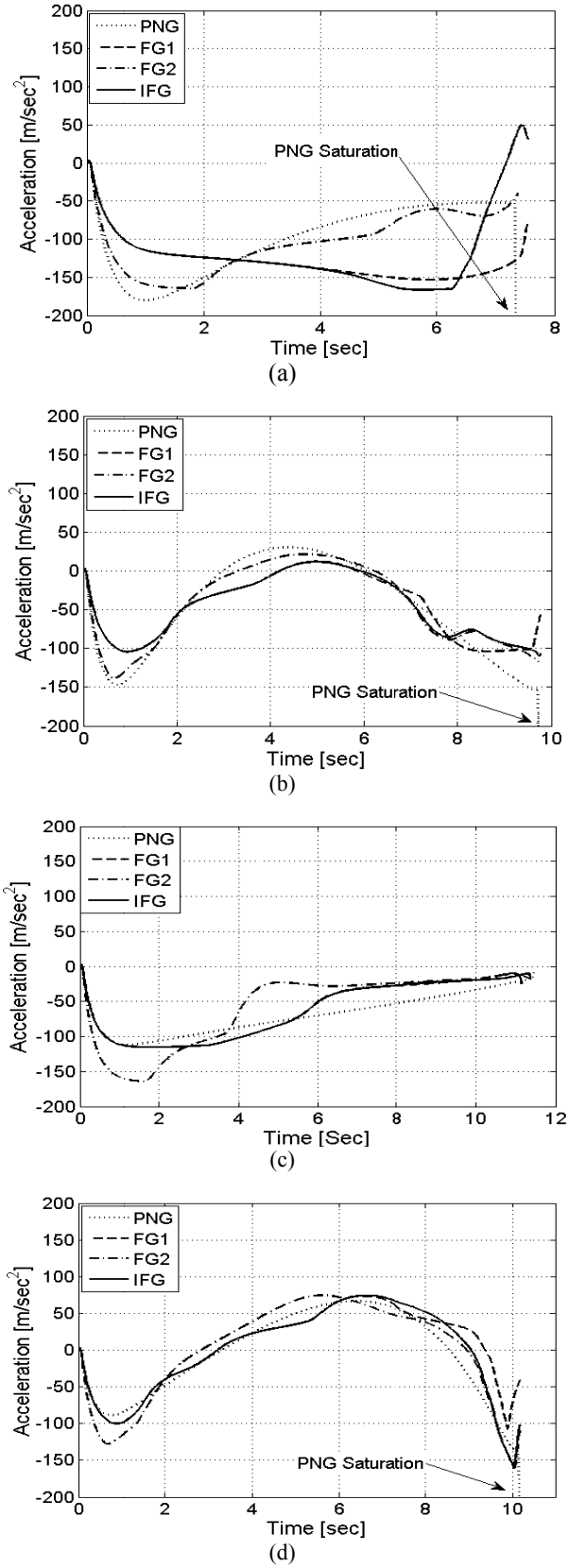

Fig. 12 Accelerations histories for different maneuvering styles. (a) Incoming Down-ward maneuvering (b) Incoming Up-ward maneuvering (c) Evading Down-ward maneuvering (d) Evading Up-ward maneuvering.

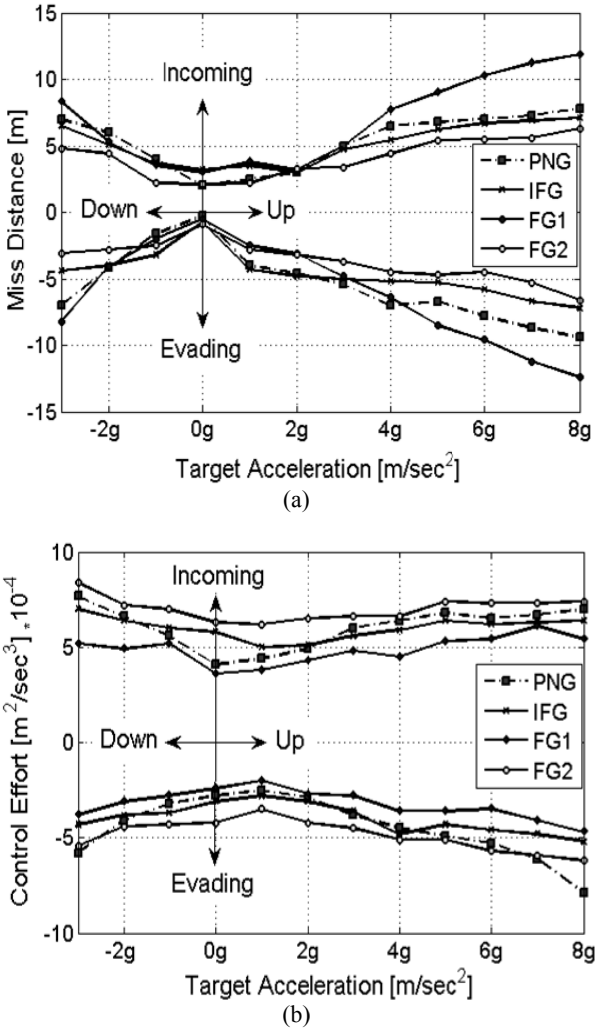

Fig. 13 M_D and C_{EFF} for the all guidance laws. (a) M_D for all guidance laws (b) C_{EFF} for all guidance laws.

Table 6 RMS of M_D and C_{EFF} for 24 scenarios.

RMS	M_D [m]	C_{EFF} [10^{-4} $m^2.sec^{-3}$]
FG1	7.86	5.36
FG2	5.13	6.84
IFG	5.43	5.84
PNG	7.21	6.52

Fig. 13 that compares PNG law with the other ones in terms of M_D and C_{Eff} verifies the results given in Table 6 and shows the following conclusions:

- This kind of fuzzy guidance laws enables to avoid the saturation caused by PNG law which, in turn, leads to increase the M_D and the C_{Eff}.
- FG1 law with low sensitivity is appropriate to conserve the C_{Eff} and shows better behavior in case of low maneuvering targets, approximately when $(|A_T| < 2g)$. On the other hand it achieves the worst when the target maneuvers sharply $(|A_T| > 2g)$.

- FG2 law with high sensitivity is appropriate when small M_D is desirable and shows good behavior for high maneuvering targets. Whereas, it causes higher C_{Eff} spending.
- IFG law which is an integral of the two prior fuzzy guidance laws seems to be perfect for all scenarios. In total, IFG law overcomes PNG law in term of both C_{Eff} and M_D.

Basing on the previous results it can be said that; three phases guidance (initial, midcourse, and terminal) are not always necessary. In fact, we can have two-phases fuzzy guidance combined of a low-sensitive phase and a high-sensitive one those have the characteristics mentioned previously. Furthermore; we can show that, under such condition low C_{Eff} demand, we can suffice to have FG1. And under the condition low M_D desire, we can use FG2, the matter that very helpful from practical point of view. That is a single set of gains is enough when a fast response is necessary.

4.1 Noise Affecting on IFG

It is well-known that measuring a target location follows a random distribution due to thermal and radar noises; therefore, white noise is added to the measured signals to account for the disturbances. Such effects can be modeled as Gaussian density function (G_{df}) declared as:

$$G_{df}(n_s) = \frac{1}{\sqrt{2\pi\sigma^2}} . e^{-\frac{(x-\mu)^2}{2\sigma^2}} \quad (9)$$

where μ is the noise mean value and σ is its standard deviation, whereas n_s is the noiseless signal. Using the MtLab function *awgn*, we add white Gaussian noise to the input signals and evaluate the RMS of M_D and C_{EFF}. The calculation is achieved for three different levels of signal-to-noise ratio (SNR). The resulted values are tabulated as shown in Table 7. This table shows that as the noise increases the missile interception capability decreases. That is because of noisy information was send to the guidance law which in turn send confused commands to the flight control system.

4.2 Additional Comparison with Other Guidance Law

The IFG is compared with an Optimal Fuzzy Logic Controller (OFLC) guidance law [24]. Table 8 shows the RMS values for the pre-examined scenarios.

The resulted values show that the IFG law overcomes the OFLC law and insures improvement of 5% and 13% regard to C_{Eff} and M_D respectively.

Fig. 14 shows trajectory and acceleration command for an arbitrary scenario ($A_T = [-3]g$). Fig. 14-a shows that the IFG law causes more bend in the trajectory because of the low sensitivity in the first stage and the high one in the second stage. Whilst Fig. 14-b shows low bends in the first stage and high bends in the second stage because of low and high sensitivities respectively.

Table 7 Performance of IFGL with noise existence.

SNR	RMS of M_D [m]	RMS of C_{EFF} [10^{-4} m^2/sec^3]
100	8.87	7.57
50	13.22	10.66
25	1162.61	5.02

Table 8 RMS values for the pre-examined scenarios.

RMS	M_D [m]	C_{EFF} [10^{-4} $m^2.sec^{-3}$]
OFLC	6.23	6.14
IFG	5.43	5.84

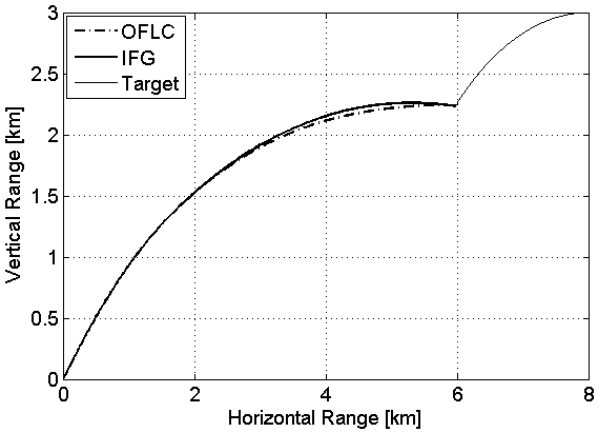

(a)

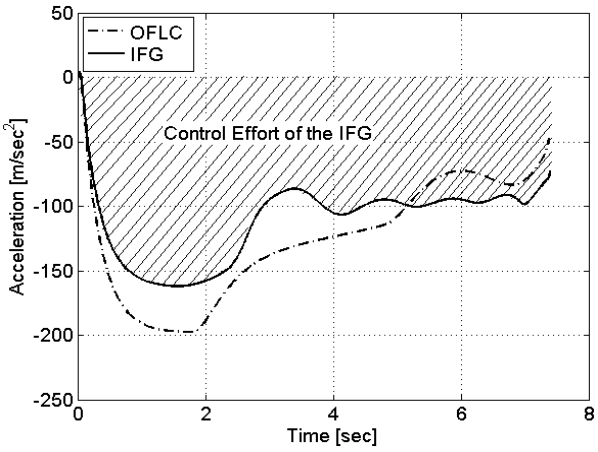

(b)

Fig. 14 Compartment of IFG law and OFLC law. (a) Trajectory (b) Acceleration command.

5 Conclusion

In this work, the possibilities of developing an IFG law with two subcomponents FG1 and FG2 is investigated. The investigation is based on a modification of classical PNG law. Simulation for variety scenarios of target maneuvering is achieved for a surface to air homing missile which dynamically described by a transfer function. RMS of the terms M_D

and C_{EFF} is calculated for all scenarios. FG1 with low sensitivity is investigated to insure small C_{EFF} values regardless of M_D whereas FG2 concerns on minimizing M_D only. The results show that both FG1 and FG2 enable the missile to track and intercept the target. Since FG1 relatively causes C_{EFF} conserving and M_D increment, FG2 diametrically does the opposite. Each of the subcomponents overweighs PNG law in one of the terms M_D or C_{EFF}. By motivating FG1 and slacking FG2 in the early flight stages, and vice versa in the last stages, an integration of the two subcomponents can be achieved. The resulted IFG shows better performance than PNG law in both terms. FSP controller secures an optimal transition between the two controllers. The FSP is optimized by an algorithm which defines when and how the transition would be done. Many cases have been examined for different scenarios. Since PNG law tends to show saturation in many scenarios, the other guidance laws do not show any saturation. Further investigations proved that the IFG shows acceptable performance in case of high SNR values. Nevertheless, further investigation maybe achieved to develop the current design in case of low SNR levels.

References

[1] B. T. Burchett, "Feedback linearization guidance for approach and landing of reusable launch vehicles", *Proceedings of the American Control Conference*, pp. 2093-2097, June 2005.

[2] C. C. Kung, F. L. Chiang and K.Y. Chen, "Design A Three-dimensional pursuit guidance law with Feedback Linearization Method", *World Academy of Science, Engineering and Technology*, Vol. 79, No. 1, pp. 136-141, 2011.

[3] F. K. Yeh, H. H. Chien and L. C. Fu, "Design of optimal midcourse guidance sliding-mode control for missiles with TVC", *IEEE Transaction on Aerospace and Electronic Systems,* Vol. 39, No. 3, pp. 824-837, 2003.

[4] R. M. Shoucri, "Closed Form Solution of Line-of-Sight Trajectory for Maneuvering Target", *AIAA Journal of Guidance, Control, and Dynamics*, Vol. 24, No. 2, pp. 408-409, 2001.

[5] C. M. Lin and Y. F. Peng, "Missile guidance law design using adaptive cerebellar model articulation controller", *IEEE Transaction on Neural Network*, Vol. 16, No. 3, pp. 636-644, 2005.

[6] V. Stepanyan and N. Hovakimyan, "Adaptive disturbance rejection controller for visual tracking of a maneuvering target", *Journal of Guidance, Control and Dynamics*, Vol. 30, No. 4, pp. 1090-1106, 2007.

[7] J. I. Lee, I. S. Jeon and M. J. Tahk, "Guidance law to control impact time and angle", *IEEE Aerospace and Electronic Systems*, Vol. 43, No. 1, pp. 301-310, 2007.

[8] V. Savkin, P. Pathirana and F. A. Faruqi, "The Problem of Precision Missile Guidance: LQR and H_∞ Frameworks", *IEEE Transactions on Aerospace and Electronic Systems*, Vol. 39, No. 3, pp. 901-910, 2003.

[9] D. Deshkar, M. Kuber and P. Parakh, "Fuzzy logic guidance law with optimized membership function", *International Journal of Computer Science and Informatics*, Vol. 1, No. 2, pp. 52-56, 2011.

[10] V. Rajasekhar and A. G. Sreenatha, "Fuzzy Logic Implementation of Proportional Navigation Guidance," *Acta Astronautica*, Vol. 46, No. 1, pp.17-24, 2000.

[11] A. Moharampour, J. Poshtan and A. Khaki-Sedigh, "A Modified Proportional Navigation Guidance for Range Estimation", *Iranian Journal of Electrical & Electronic Engineering*, Vol. 4, No. 3, pp.115-126, July 2008.

[12] A. Moharampour, J. Poshtan and A. Khaki-Sedigh, "A Modified Proportional Navigation Guidance for Accurate Target Hitting", *Iranian Journal of Electrical & Electronic Engineering,* Vol. 6, No. 1, pp. 20-28, 2010.

[13] G. Siouris, *Missile Guidance and Control Systems,* Springer Verlag, New York, 2004.

[14] P. Zarchan, *Tactical and Strategic Missile Guidance*, Third Edition, AIAA, Chapter 6, 2002.

[15] C. L. Lin and Y. Y. Chen, "Design of Fuzzy Logic Guidance Law against High Speed Target", *Journal of Guidance, Control and Dynamics*, Vol. 23, No. 1, pp. 17-25, 2000.

[16] J. S. R. Jang, "Adaptive-Network-Based Fuzzy Inference system", *IEEE Transactions on Systems, Man, and Cybernetics*, Vol. 23, No. 3, pp. 665-685, 1993.

[17] W. V. Leekwijck and E. E. Kerre, "Defuzzification: criteria and classification", *Fuzzy Sets and Systems*, Vol. 108, No. 2, pp. 159-178. 1999.

[18] J. Lindblad and N. Sladoje "Feature Based Defuzzification at Increased Spatial Resolution", *Proc., of 11th Intern. Workshop on Combinatorial Image Analysis, Berlin, Germany, Lecture Notes in Computer Science,* LNCS. 4040, pp. 131-143, 2006.

[19] J. S. R. Jang, "Fuzzy Modeling Using Generalized Neural Networks and Kalman Filter Algorithm", *Proc. of the Ninth National Conf. on Artificial Intelligence (AAAI-91)*, pp. 762-767, July 1991.

[20] M. L. Padma, V. C. Veera and N. R. Sivarami, "Application of Fuzzy and ABC Algorithm for DG Placement for Minimum Loss in Radial Distribution System", *Iranian Journal of Electrical & Electronic Engineering,* Vol. 6, No. 4, pp. 248-256, 2010.

[21] C. L. Lin, H. Z. Hung, Y. Y. Chen and B. S. Chen, "Development of an Integrated Fuzzy logic based missile guidance law against high speed target", *IEEE, Transaction on Fuzzy System*, Vol. 12, No. 2, pp. 157-169, 2004.

[22] S. Chakraborty and C. Yeh, "A Simulation Based Comparative Study of Normalization Procedures in Multi-attribute Decision Making", *The 6th WSEAS Int. Conf. on Artificial Intelligence, Knowledge Engineering and Data Bases, Corfu Island, Greece*, pp. 102-109, 2007.

[23] L. L. Chun, C. K. Tzu and T. W. Meng, "Design of a Fuzzified Terminal Guidance Law", *International Journal of Fuzzy Systems*, Vol. 9, No. 2, pp. 110-115, 2007.

[24] S. Li and L. Yuan, "Design of Fuzzy Logic Missile Guidance Law with Minimal Rule Base", *Sixth International Conference on Fuzzy Systems and Knowledge Discovery*, pp. 176-180, 2009.

Labeed Hassan was born in Syria, 1977. He received B.Sc. and M.Sc. in electrical engineering from the electrical engineering department of Aleppo University, Syria, in 2000 and 2007 respectively. He is currently a Ph.D. candidate in the Department of Aerospace Engineering at Maleke Ashtar University of Technology, Tehran, Iran.

Seyed Hossein Sadati is an Assistant Professor in the Department of Aerospace Engineering at Maleke Ashtar University of Technology, Tehran, Iran. He received his Ph.D. in Aerospace Engineering from Amirkabir University in 2008. He has published more than 30 journal and conference papers in the area of Aerospace Engineering. His current research interests include the control system design for aircraft, trajectory optimization, nonlinear control, optimal control, neural network and fuzzy Control.

Jalal Karimi is an Assistant Professor in the Department of Aerospace Engineering at Maleke Ashtar University of Technology, Tehran, Iran. He received his Ph.D. in Aerospace Engineering from Sharif University of Technology in 2012. His current research interests are motion planning, heuristic optimization and guidance system design.